

## Ideal core MHD stability in operational scenarios in JT-60SA

R. Coelho<sup>[1]</sup>, J. Garcia<sup>[2]</sup>, F. Liu<sup>[2]</sup>

[1] Instituto de Plasmas e Fusão Nuclear, Instituto Superior Técnico, Universidade de Lisboa, 1049-001 Lisboa, Portugal

[2] CEA, IRFM, F-13108 Saint-Paul-lez-Durance, France

### I – Introduction

The scientific work programme of the JT-60SA tokamak foresees several operational scenarios [1] at normalised plasma beta close or larger than 3, ranging from full  $I_p$  inductive at 41MW heating power with different heights in the pedestal density, hybrid like scenarios with 37MW of heating power and strongly reversed shear scenarios (heating power larger than 30MW) in a full non-inductive current operation. While on the pedestal it is largely anticipated that all scenarios are peeling-balloonning (PB) unstable, the core MHD stability is less straightforward except when the plasma scenarios are sawtoothing. In particular, large pressure gradients may give rise to local ballooning-infernal or kink modes resonant with magnetic surfaces close to the  $q=1$  magnetic surface or possible minima in the safety factor  $q$  profile. In this work we investigate the ideal core MHD stability of the foreseen scenarios and present a comprehensive analysis of the MHD spectra characteristic from each scenario. The background plasma and equilibria stem from modelling done using the CRONOS suite using dedicated models for core particle and heat transport e.g. GLF23 and CDBM [2,3]. Such models lack of some characteristics expected to be important in JT-60SA, e.g. the impact of electromagnetic effects on turbulence, yet they were used as a first step towards a full prediction of scenarios in JT-60SA.

### II – Modelled plasma scenarios

The operational scenarios address fundamentally fully inductive scenarios at low (Scenario 2) and high (Scenario 3) electron plasma density, a hybrid scenario (Scenario 4) and an advanced scenario with strong core magnetic shear reversal (Scenario 5). The plasma current and toroidal magnetic field are summarized in Table I

	<b>Scenario 2</b>	<b>Scenario 3</b>	<b>Scenario 4 (CDBM)</b>	<b>Scenario 5</b>
<b><math>I_p / B_T</math></b>	5.5MA / 2.25T	5.3MA / 2.05T	3.6MA / 2.28T	2.3MA / 1.72T

Table I – Summary plasma current and toroidal magnetic field for the scenarios

Figure 1 summarizes the four scenarios showing both the equilibrium plasma cross section and flux surfaces as well as some fundamental radial plasma profiles. With exception of

Scenario 5, the q-profile hovers around 1 about the magnetic axis. Although scenarios 2 and 3 capture the characteristic post-sawtooth crash flattening of the q-profile around 1, for scenario 3 a slight shear reversal with a double q=1 surface exists at mid-radius.

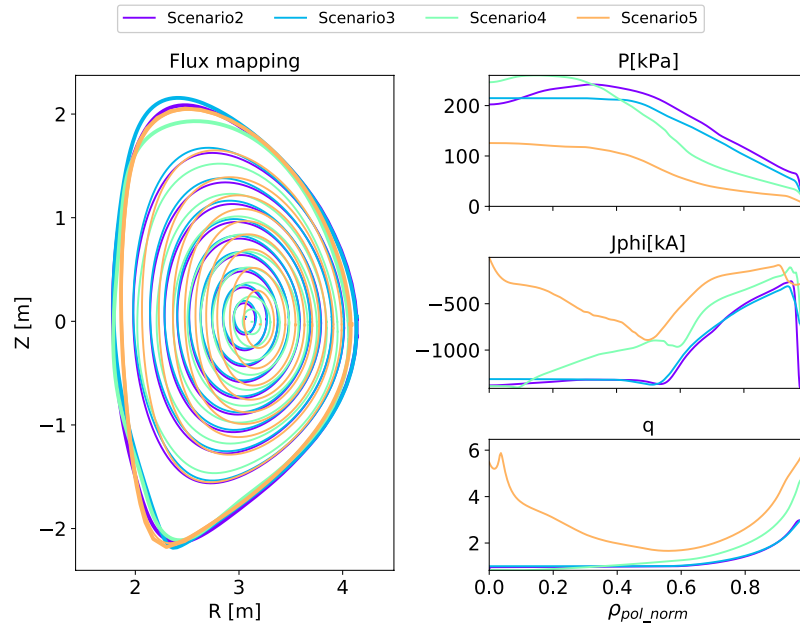


Figure 1 – Plasma cross section and flux surfaces for the 4 operational scenarios (left). Radial profiles for the plasma pressure (top-right), toroidal current density (middle-right) and safety factor (bottom-right). The radial coordinate is the squared root of the normalized poloidal magnetic flux.

### III – Stability analysis

The stability analysis was performed using the EQSTABIL workflow developed within EUROfusion [4] and implemented using the IMAS modelling infrastructure [5]. The high resolution equilibria were obtained using either the HELENA [6] or CHEASE [7] codes and the ideal MHD stability was calculated using the ILSA [8] code. In scenario 2 the stability is dominated by the  $q=1$  magnetic surface with kink unstable modes with maximum growth rate for toroidal mode number  $N=8$  (see Figure 2-left). In addition, all modes essentially resonate at the  $q=1$  magnetic surface, evidenced both by the

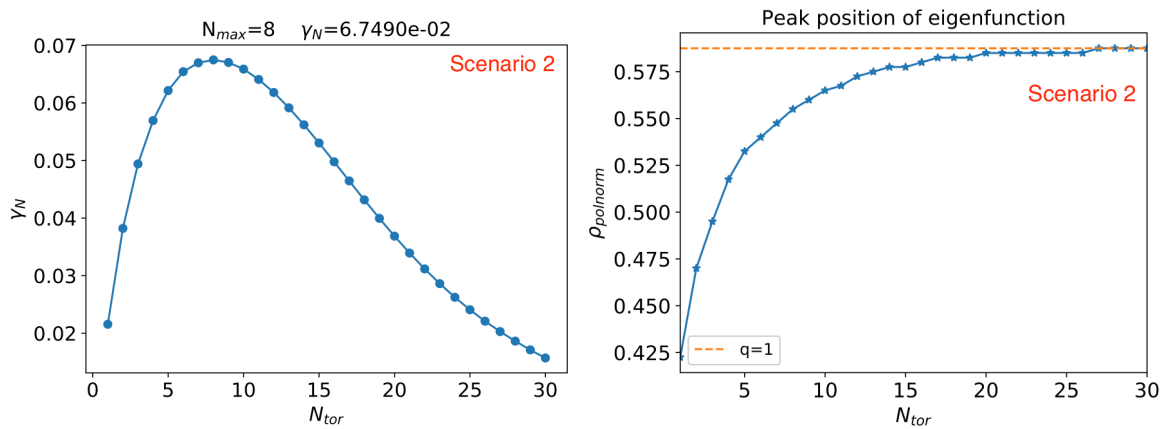


Figure 2 - Normalised growth rate normalized to the Alfvén frequency dependence with toroidal mode number (left) and radial peak location of the eigenfunction for each toroidal mode number ( $N_{tor}$ ).

dominant poloidal harmonic ( $m$ ) of the eigenfunction (always  $m=n$ ) and by the “radial” location of the peak mode amplitude, progressively closer to the  $q=1$  surface as the toroidal

mode increases (see Figure 2-right). Considering scenario 3, it features a double magnetic surface  $q=1$  located at  $\rho_{polnorm} \sim 0.495/0.534$ , on axis  $q(0)=1.001$  and the minimum safety factor  $q_{min}(0.518)=0.999$  (see Figure 3-right). With the modes located within the  $q_{min}$  and

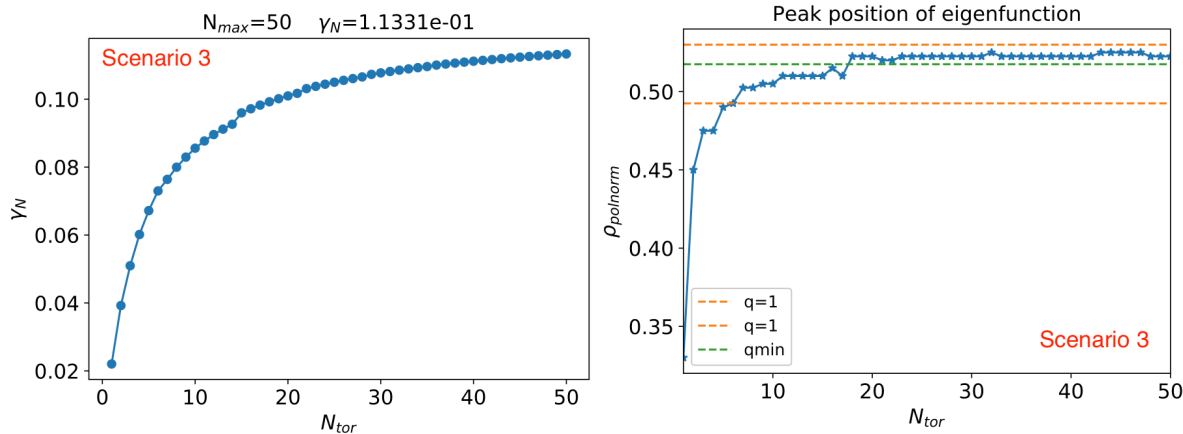


Figure 3 - Normalised growth rate dependence with toroidal mode number (left) and radial peak location (right) of the eigenfunction for each toroidal mode number ( $N_{tor}$ ).

outer  $q=1$  magnetic flux surfaces as shown in Figure 3-right, shear stabilization contribution is minimised thus enabling increasing growth rate with toroidal mode number. Although the highest pressure gradient (with the exception of the pedestal region) is also within the same  $q_{min}$  region, it is possible that it's nonetheless insufficient to drive infernal modes.

In scenario 4, there is an ITB in the ion energy channel concomitant with the large pressure gradient at  $\rho_{polnorm}=0.56$ . As expected, with  $q(0)<1$ , the  $n=1$  mode is kink unstable and one quickly transits to a family of modes that are clearly aligned to the highest pressure gradient region, as illustrated in Figure 4. Other unstable modes at lower growth rate (also ballooning character) are identified, resonant between the  $q=1$  and highest pressure gradient

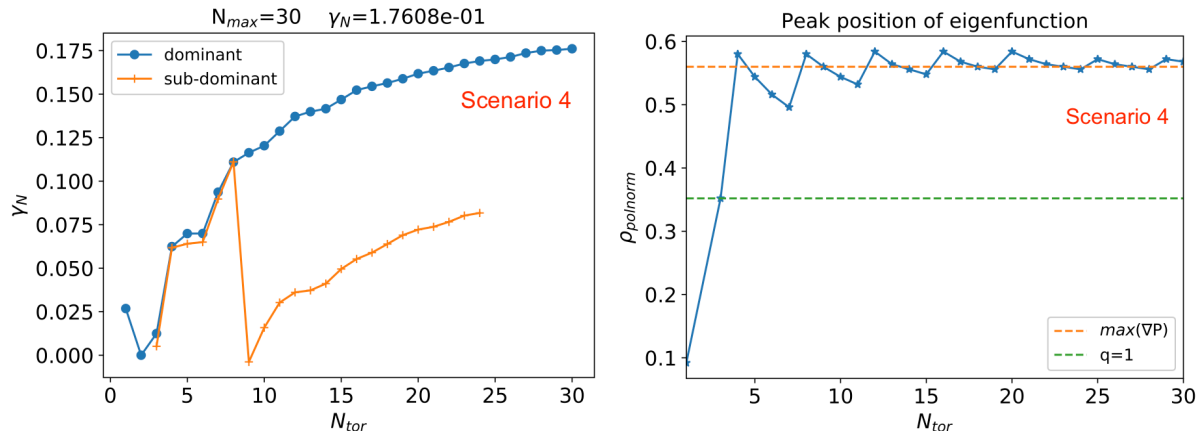


Figure 4 - Normalised growth rate dependence with toroidal mode number (left) and radial peak location of the eigenfunction for each toroidal mode number ( $N_{tor}$ ). Highest pressure gradient and  $q=1$  radial position are also indicated.

surface and with perturbed radial velocity slightly odd about the latter surface.

Finally, in scenario 5 the positive shear region is as anticipated MHD unstable, with strongly unstable ballooning modes with highest mode amplitude region  $\rho_{polnorm} \sim 0.62$  as observed in Figure 5. Although the pressure gradient at the modes location is only 55% of the peak pressure gradient value at mid-radius ( $\sim 68 \text{ kPa/Wb}$  at  $\rho_{polnorm} \sim 0.5$ ), magnetic shear is no longer zero which grants access to the unstable region. No low-n infernal type modes are observed close to the  $q_{\min}$  magnetic surface.

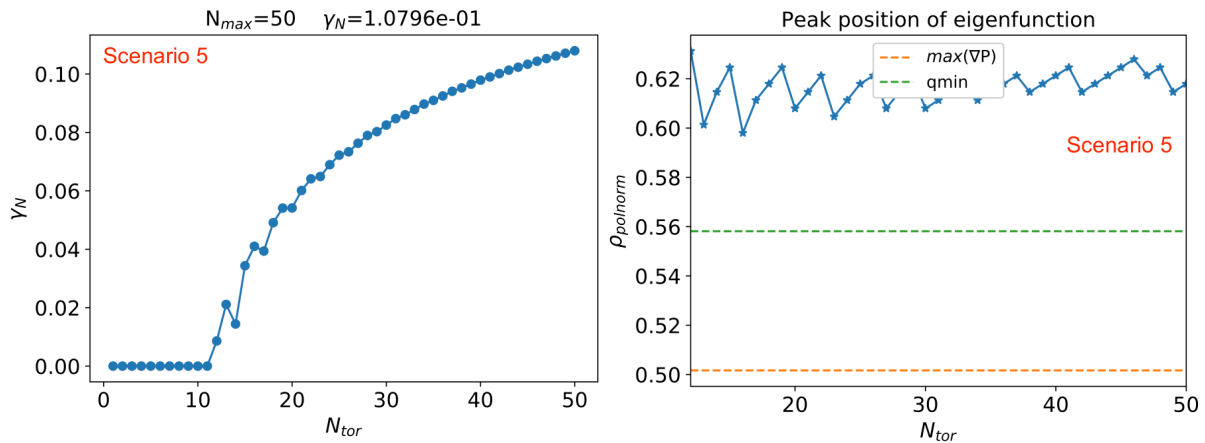


Figure 5 - Normalised growth rate dependence with toroidal mode number (left) and radial peak location of the eigenfunction for each toroidal mode number ( $N_{tor}$ ). Highest pressure gradient and  $q_{\min}$  radial position are also indicated.

#### IV – Conclusions

The ideal/internal MHD stability of the JT-60SA operational scenarios obtained from modelling done using the CRONOS suite using dedicated models for core particle and heat transport e.g. GLF23 and CDBM was addressed. It was found that while the fully inductive scenarios are mostly kink unstable in the vicinity of the  $q=1$  surface, as large pressure gradients become more evident in the advanced scenarios, ballooning like modes become strongly unstable, with occasionally more than one unstable branch being identified.

#### Acknowledgements

This work has been carried out within the framework of the EUROfusion Consortium, funded by the European Union via the Euratom Research and Training Programme (Grant Agreement No 101052200 — EUROfusion). Views and opinions expressed are however those of the author(s) only and do not necessarily reflect those of the European Union or the European Commission. Neither the European Union nor the European Commission can be held responsible for them. IPFN activities received financial support from “Fundação para a Ciência e Tecnologia” through projects UIDB/50010/2020 and UIDP/50010/2020

#### References

- [1] M Yoshida et al 2022 Plasma Phys. Control. Fusion **64** 054004; [2] L. Garzotti et al 2018 Nucl. Fusion **58** 026029; [3] J. Garcia et al 2014 Nucl. Fusion **54** 093010; [4] <https://wpcd-workflows.github.io/es.html>; [5] F. Imbeaux et al, Nucl. Fusion **55** 12 (2015) 123006 [6] G. Huysmans et al., Int. J. Mod. Phys. C 2 371, (1991); [7] H. Lutjens et al, Comput.Phys.Comm **97** (1996) 219; [8] R. Coelho et al, 42<sup>nd</sup> EPS Conference Lisbon (2015) - <http://ocs.ciemat.es/EPS2015PAP/pdf/P4.178.pdf>